CHAPTER 7

AN OPTIMIZED CONVOLUTIONAL NEURAL NETWORK-BASED ENSEMBLE CLASSIFICATION AND REGRESSION FRAMEWORK FOR CLASSIFYING THE STAGES OF DIABETIC RETINOPATHY

7.1 Introduction

The aim of the SGAN-ECR model discussed in Chapter 6 was to present an effective multi-class classification of DR stages with a variety of images with high contrast and low saturation. The SGAN-ECR model discussed in Chapter 6 assigns hyperparameter values manually. Random hyperparameter values lead to increased error rates and subjective decisions. In this chapter, SGAN-OECR model aims to improve the classification performance of DR stages using an enhanced optimization technique that assigns the best set of hyper-parameter values automatically. An Enhanced Mine Blast Optimization Algorithm (EMBOA) is proposed for optimizing the hyper-parameter values of MSA-ResNet Structures. Learning rate, momentum, batch size, convolutional layer, kernel size, activation function, filter size, dropout and the number of epochs is the hyper-parameters considered to optimize the CNN-based MSA-ResNet Classification and Regression model. The model is trained using SGAN-generated images along with original dataset images. The trained model is identified with test images abnormalities like DR lesions. The MLP classifier of MSA-ResNet classifies the DR stages. The accuracy of the classifier depends on allocating parameters values. Therefore, an EMBOA is proposed to optimize the MSA-ResNet hyper-parameters in SGAN-ECR model.

The following sections in this chapter are organized as follows. A detailed description related to the SGAN-OECR model to optimize hyper-parameters in MSA-ResNet structure, and the various hyper-parameters are discussed. The schematic representation of the SGAN-OECR model and an Enhanced Mine Blast Optimization Algorithm are explained in the subsequent sections. Experimental results are analyzed based on the performance metrics, and the outcome analysis and assessment of the proposed technique are presented conclusively.

7.2 The Proposed SGAN-OECR Model

This section discusses the schematic representation of the proposed SGAN-OECR model, the configuration of the hyper-parameters for the MSA-ResNet structure, and an Enhanced Mine Blast Optimization Algorithm to tune the hyper-parameters.

7.2.1 SGAN-OECR Model for DR stage classification

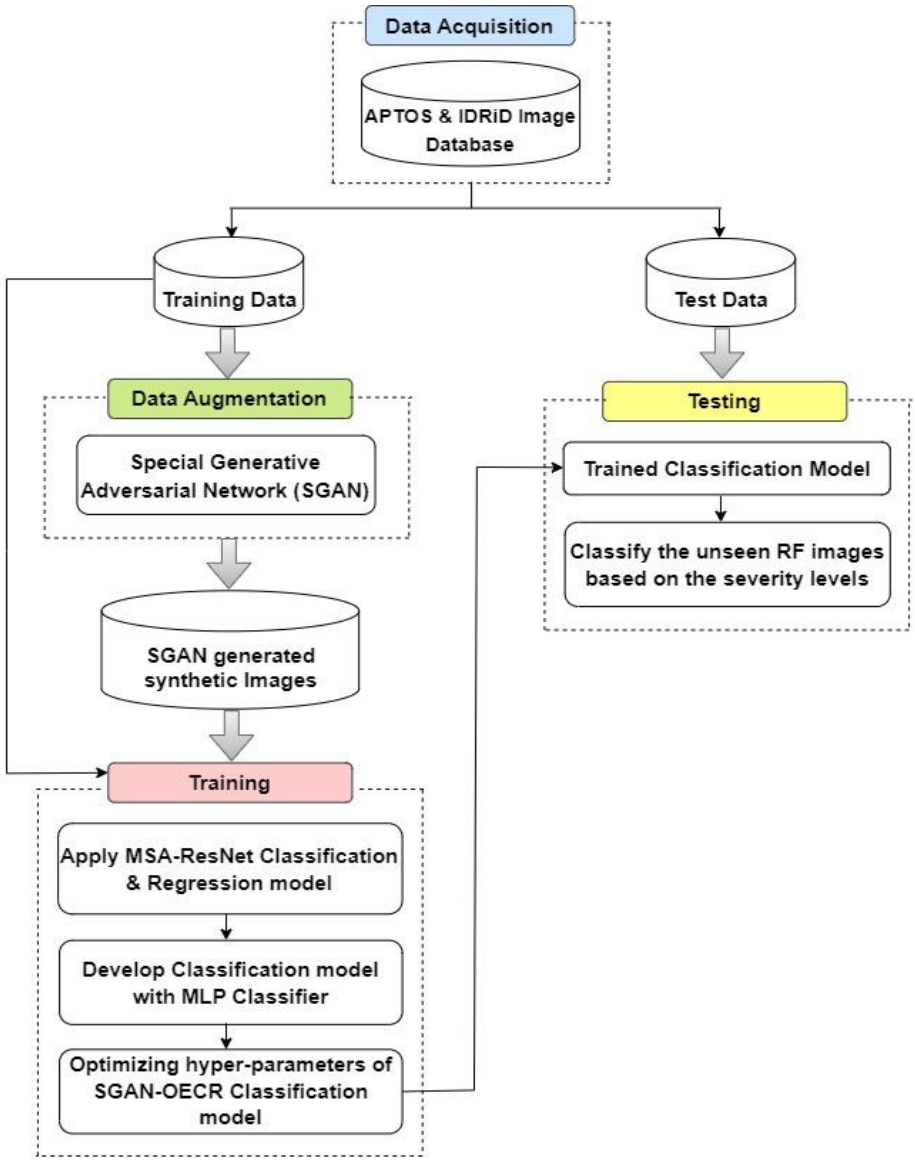

Figure 7.1: SGAN-OECR Model Workflow for DR Stage Classification

The proposed SGAN-OECR model for DR stage classification includes optimizing the hyper-parameters of the SGAN-ECR model to maximize its classification performance

based on the DR severity levels. In the SGAN-ECR model, realistic synthetic retinal images were generated using SGAN. The dataset images, along with SGAN-generated images, were used to train MSA-ResNet classification and regression structure. The learned features from the classification and regression model are then concatenated, and with the help of the MLP classifier, the retinal fundus images are classified based on DR severity levels. The SGAN-ECR model was found to be effective as the model was trained on more realistic images that had varied features. To improve the classification accuracy further, the hyper-parameters of the SGAN-ECR model are optimized using an EMBOA. The generated model is implemented to test the illustrations and categorize DR stages. Figure 7.1 shows the workflow of the SGAN-OECR Model to categorize different stages of DR disease based on severity levels. The subsequent sections define these diverse processes.

7.2.2 MSA-ResNet Structure for hyper-parameters tuning

The framework aims to implement an efficient technique for automatically optimizing the hyper-parameters. The estimation of hyper-parameters like layer count, filter count, filter size, FC layer count and hidden units in FC layer count are presented. Equation (7.1) is the set of hyper-parameters.

$$H = H_{conv}, H_{fc} \tag{7.1}$$

Where H_{conv} denotes the convolution layer parameter, H_{fc} denotes the FC layer parameter.

The Equation (7.2) defines the convolution layer parameter.

$$H_{conv} = \{c_0, \dots, c_{N-1}\} \tag{7.2}$$

Where c_N denotes the number of convolution layer

Equation (7.3) represents the convolutional layer in the a^{th} layer with two tuples.

$$c_a = (d_{count}, d_{size}) \tag{7.3}$$

Where d_{count} denotes the filter count, d_{size} denotes the filter size in the a^{th} layer.

Equation (7.4) represents the set of the fully connected layers:

$$H_{FC} = t_0, t_{k-1} \tag{7.4}$$

Where t denotes hidden FC layer (a^{th} layer), k denotes FC layer count. Q denotes MSA-ResNet configuration. To identify and configure $q \in Q$ to obtain minimum error rate classification. (Cer) denotes classification error rate. The hyper-parameter values are optimized using EMBOA technique to enhance accuracy. The optimization of the parameters minimizes the computer resources utilization. Table 7.1 illustrates the configuration of hyper-parameter values and their range in the MSA-ResNet structure.

Table 7.1: MSA-ResNet Hyper-parameters and their range

S.No.	Hyper-parameters	Range
1	Learning Rate	Min. value – 0.001, max. value-0.1
2	Momentum	Min. value – 0.9, max. value-0.99
3	Batch size	Min. value – 32, max. value-256
4	Convolutional Layer	Min. value – 5, max. value-516
5	Kernel size	[(2,2), (3,3), (5,5), (6,6)]
6	Activation function	ReLU, Sigmoid, LReLU
7	Filter size	Min. value – 64, max. value-256
8	Dropout	Min. value – 0.1, max. value-0.9
9	No. of epochs	Min. value – 25, max. value-300

7.2.3 Schematic representation of SGAN-OECR Model

The schematic representation of the SGAN-OECR model is represented in Figure 7.2. The SGAN-OECR includes the SGAN and ECR structures. SGAN comprises pixel-2-pixel GAN and patch-GAN representing the quality images. The related training model from the classifier is suitable for obtaining high-quality images.

The ECR section consists of MSA-ResNet regression and classification for feature extraction and DR stage classification. The hyper-parameters in the MSA-ResNet model are optimized with the help of the optimization algorithms. In this study, an EMBOA is used to optimize the hyper-parameters. The MBOA algorithm is an evolutionary algorithm that aids in the selection of appropriate hyper-parameters to enhance accuracy with a minimum number of iterations.

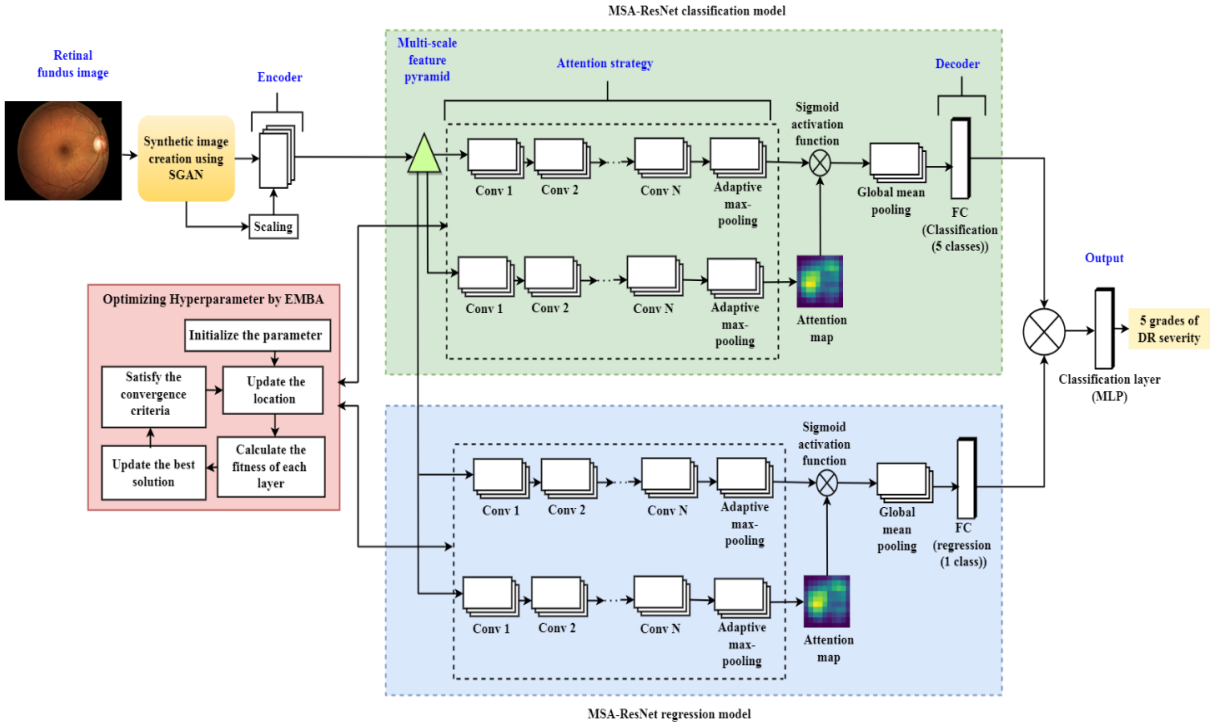

Figure 7.2: Schematic Representation of SGAN-OECR Model

7.2.4 Enhanced Mine Blast Optimization Algorithm (EMBOA)

MBOA comes under metaheuristic techniques (Sadollah *et al.*, 2013) used in the optimization field. This algorithm is mostly used in engineering problems with discrete variable structures. Meta-heuristics can often find optimal solutions with less computational effort than optimization algorithms. It excels in exploring complex, multi-dimensional search spaces where traditional methods may struggle. Meta-heuristic algorithms inherently balance exploration and exploitation. They explore the search space to discover new regions while also exploiting promising areas. This ability to strike a balance is crucial for effective hyper-parameter optimization, where the goal is to find the global optimum rather than settling for a local one.

In this study, EMBOA is used to optimize the hyper-parameters of the SGAN-OECR model. MBOA is inspired by the landmine detonation process. During landmine explosion, the shrapnel collides with nearby landmines in the explosion area. This process eliminates the other landmines. Thus, to identify an optimal solution, initial blasting point and the volume of collision is identified to eliminate prevailing mines in that area. Later, the first-time explosion

initial point (X) is identified. The shrapnel fragments are distributed across the search area. Other explosions occur with respect to the pointer. Collisions happen between the shrapnel fragments and other landmines. Every explosion occurs at diverse points which is based on the previous blasts and each point (X) is estimated and represented as F(x) (Sadollah *et al.* 2015).

In MBOA technique, an initial population is assumed as an optimal solution and further the first explosion is generated. The population size represents shrapnel fragment count (Sadollah *et al.*, 2013). Generally, metaheuristic algorithms have global search (exploration) phase and local search (exploitation) phase (Sadollah *et al.*, 2014). The shrapnel movement in multiple new locations represents exploration and utilization of existing resources in the identified locations represents exploitation. In Figure 7.3 color lines represent exploration and black lines represents exploitation.

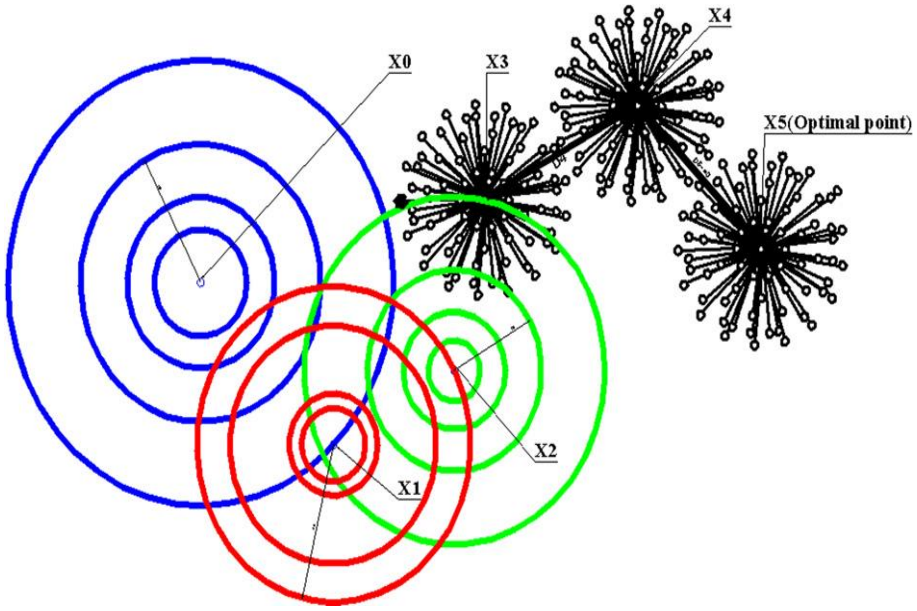

Figure 7.3: Exploration (color lines) and exploitation (black lines) phases in MBOA

MSA-ResNet model contains a set of hyper-parameters to configure Q. Initial population generation is represented in Equation (7.5).

$$f(Q) = f(X) = \frac{1}{1+|Cer|} \tag{7.5}$$

Where $f(Q)$ denotes the fitness function for the configuration set Q. The fitness $f(X)$ denotes exploitation shot point X. Here, X represents configuration set Q. The configuration

of hyper-parameters in MSA-ResNet is denoted as $X.Cer$ denotes the classification error for the selected configuration parameters of MSA-ResNet model.

The various steps involved in EMBOA for the MSA-ResNet model are discussed below:

1. Initialization

The initial shot location (hyper-parameters set) determines the search space, and the initial shot location is selected randomly. The lower limit parameters are the original location of the shot, and the next shot is estimated as represented in Equation (7.6).

$$X_0^{current} = \ell b + rand * (ub - \ell b) \tag{7.6}$$

Where $X_0^{current}$ denotes the initial explosion location, ℓb and ub denote the lower and upper bound of the search space.

2. Iteration Process

The next explosion location is estimated as represented in Equation (7.7)

$$X = X_T, T = 1, 2, 3, .., n_d \tag{7.7}$$

Where n_d denotes the search space of position X.

The additional landmine locations are identified by shrapnel as represented in Equation (7.8)

$$X_{n+1}^b = X_{z(n+1)}^b + \exp\left(-\sqrt{\frac{T_{n+1}^b}{d_{n+1}^b}}\right) * X_n^b \tag{7.8}$$

Where $n = 0,1,2,$ ...d, $X_{z(n+1)}^b$ denotes the location of a mine exploding, T_{n+1}^b and d_{n+1}^bdenotes the orientation and range of shrapnel pieces, and b denotes the total number of initial shot locations. The equation (7.9) determines the location of the exploding landmine.

$$X_{z(n+1)}^b = d_{n+1}^b \times r \times \cos(\theta) \tag{7.9}$$

Where r is the random integer [0,1], θ denotes the shrapnel angle corresponding to $360/Nb$

Shrapnel distance and direction are computed using Equation (7.10) and Equation (7.11). The location of the exploded landmine is estimated by using Equation (7.9).

$$d_{n+1}^{b} = \sqrt{(X_{n+1}^{b} - X_{n}^{b})^{2} \quad + \quad (F_{n+1}^{b} - F_{n}^{b})^{2})} \tag{7.10}$$

$$T_{n+1}^{b} = \frac{F_{n+1}^{b} - F_{n}^{b}}{X_{n+1}^{b} - X_{n}^{b}} \tag{7.11}$$

Where F denotes the fitness function of X. The exploitation uses current solution's fitness value.

3. Exploration Phase

The exploration process in the search space with minimum and maximum distances. The process depends on the number of iteration counted. The process is represented in Equation (7.12) and Equation (7.13).

$$d_{n+1}^{b} = X_{n}^{b} * r^{2} \tag{7.12}$$

$$X_{z(n+1)}^{b} = d_{n+1}^{b} * \cos(\theta) \tag{7.13}$$

4. Exploitation Phase

The exploitation process is performed by an exploration factor (γ) and iteration count(b). Constant value is minimized, and fragment distance is decreased in an explosion. The eliminated distance is estimated using Equation (7.14).

$$X_{n}^{b} = \frac{\gamma_{n-1}^{b}}{\exp(\frac{b}{\varepsilon})} \tag{7.14}$$

5. Updating Best Solution

Changes in the length between current exploded location is $X_{z(n+1)}^{b}$ and the solution X_{best} is improved using Equation (7.15) and Equation (7.16).

$$X_{n+1}^{b} = X_{z(n+1)}^{b} + exp(-\sqrt{\frac{1}{ED}}) \times r \otimes \{X_{best} - X_{z(n+1)}^{b}\}, j = 1,2, \ldots n \tag{7.15}$$

$$ED = \left[\sum_{i=1}^{T} (X_{best} - X_{z(n+1)}^{b})^{2}\right]^{1/2} \tag{7.16}$$

Where, ED denotes Euclidean distance between an optimal solution X_{best} and current explosion point $X_{z(n+1)}^{b}$ with T dimensions. The pseudo-code of the SGAN-OECR model is presented. Table 7.2 illustrates the EMBOA parameter settings.

Table 7.2: EMBOA parameter settings

Parameter	Value
Upper bound	1
Lower bound	0
Maximum distance	2
Number of iterations	200
Population size	20
Constant	0.1
Exploration Factor	0.5

The upper and lower bound values are set as 0 and 1, in which the optimization problem involves variables constrained within the range [0, 1], which is common in many optimization problems, particularly in those involving probabilities or percentages. The maximum distance value is set as 2, which implies that the algorithm allows for relatively large steps in the search space, which can facilitate efficient exploration without risking excessive exploration that might lead to poor convergence or premature convergence. The number of iterations is set as 200, which provides a sufficiently large number of iterations for the optimization algorithm to converge to a satisfactory solution. This number is often determined based on experimentation and balancing the trade-off between computational resources and optimization performance. The population size is set as 20, which strikes a balance between exploration capabilities and computational efficiency.

It is large enough to promote diverse exploration but not excessively large enough to burden computational resources. A higher value of γ promotes more exploration during the optimization process, which can help in escaping local optima and searching for diverse regions of the search space. Conversely, a lower value of γ would prioritize exploitation, focusing more on refining and exploiting known promising regions. Common values for γ range between 0 and 1, where 0 indicates pure exploitation (no exploration), and 1 indicates pure exploration (no exploitation). Depending on the problem and algorithm, a value around 0.5 might provide a balanced trade-off between exploration and exploitation. The smaller values of ε lead to smaller steps in the search space during explosions, resulting in finer exploration. Conversely, larger values of ε allow for larger steps, which might facilitate faster

exploration but with potentially less precision. The choice of ε is often problem-dependent and might require some experimentation. The common values for ε are typically small positive real numbers, such as 0.01 or 0.1, but the exact value would need to be adjusted based on the scale and characteristics of the search space.

Pseudo code: The Proposed SGAN-OECR model for DR Stage Classification

Input: *Retinal Fundus images from APTOS & IDRiD dataset along with SGAN generated synthetic images* $I_1, \dots, I_n$

Output: *Different DR classes/stages*

Begin

Initialize primary parameters $N_d, \gamma, \varepsilon, \mathcal{ub}, \mathcal{lb}, p_{max}$*;*

$While(p < p_{max})$*;* $p \leftarrow p + 1$*;*

Step 1: *Initialize the initial shot location.*

Step 2: *Create other shrapnel pieces and update locations; Compute distance and direction of shrapnel*

Step 3: *Estimate the fitness function and update the distance and direction of shrapnel pieces using the MSA-ResNet model. The highest fitness value is considered the best location with shrapnel pieces;*

Step 4: *The location of the shrapnel pieces is enhanced by the exploration and exploitation phase. The process stops if the terminating criteria is met else shrapnel pieces process is generated;*

Step 5: *The best location of the shrapnel pieces is stored else replace the location of shrapnel pieces with another location;*

end while;

Step 6: *Choose the highest fitness value with the best shrapnel piece location. Get the trained model from the MSA-ResNet classification.*

Step 7: *Classify test images (DR severity grades) using trained model;*

End.

7.3 Result Analysis

This section discusses about the results of the SGAN-OECR model. The proposed model is evaluated on APTOS and IDRiD are described. The proposed and the existing

classification methods comparison and the confusion matrices are elaborated. The test results for the SGAN-OECR model are discussed.

7.3.1 Result Analysis of SGAN-OECR model on the APTOS dataset

The performance metrics of the proposed SGAN-OECR model are trained on APTOS and IDRiD, to classify the stages of DR. Multi-class classification is carried out, and the dataset is classified into five classes starting from 0 to 4. In the APTOS dataset, out of 3662 training samples, 10% of the samples are considered for test data. Table 7.3 illustrates the existing models for DR stage classification on the APTOS dataset. Table 7.4 shows the comparison of the proposed models for DR stage classification on the APTOS dataset. Accuracy metric is one of the frequently used metrics, and the other metrics are also presented. The accuracy percentage obtained by the MSA-ResNetGB is 94.40 and SGAN-ECR is 97.81. The accuracy percentage obtained by the SGAN-OECR model is 98.21, which is superior to the other models considered.

Figure 7.4 shows the confusion matrix of the SGAN-OECR model on the APTOS dataset. The matrix illustrates sample distribution by classes and the ratio of accurate classification and misclassified samples. For example, the precisely identified sample count is 357 for class 0 (no DR). For class 1(mild DR), the precisely identified sample count is 78. For class 2 (moderate DR), the precisely identified sample count is 195. For class 3 (Severe DR), the precisely identified sample count is 34 and finally, for class 4 (PDR), the precisely identified sample count is 57.

Table 7.3: Existing models for DR Stage Classification on the APTOS 2019 dataset

Reference	Classification Technique	Accuracy (%)	Precision (%)	Recall (%)	F1-Score (%)
Sikder N et. al(2021)	DT-EL	86.81	87.31	87.74	87.51
Saeed F et.al(2021)	ResNetGB	88.40	88.72	88.40	88.47
Khan Z et. al(2021)	VGG-NIN	87.65	92.86	92.86	92.86
Abdelmaksoud E et.al(2021)	U-Net	87.37	91.76	93.98	92.86
Yao Z et. al(2022)	Funswim	88.89	92.59	94.94	93.75

Reference	Classification Technique	Accuracy (%)	Precision (%)	Recall (%)	F1-Score (%)
Ullah N et.al(2022)	DCNN	89.47	94.12	94.12	94.12

Table 7.4: Comparison of the Proposed Models for DR Stage Classification on the APTOS 2019 dataset

Reference	Classification Technique	Accuracy (%)	Precision (%)	Recall (%)	F1-Score (%)
SrinivasanV & Rajagopal V (2022)	MSA-ResNetGB Model	94.40	94.53	94.40	94.43
Valarmathi S and Vijayabhanu R (2022)	SGAN-ECR model	97.81	95.95	97.98	96.90
Valarmathi Srinivasan & Vijayabhanu Rajagopal (Proposed - 2023)	**SGAN-OECR Model**	**98.21**	**98.12**	**96.42**	**97.86**

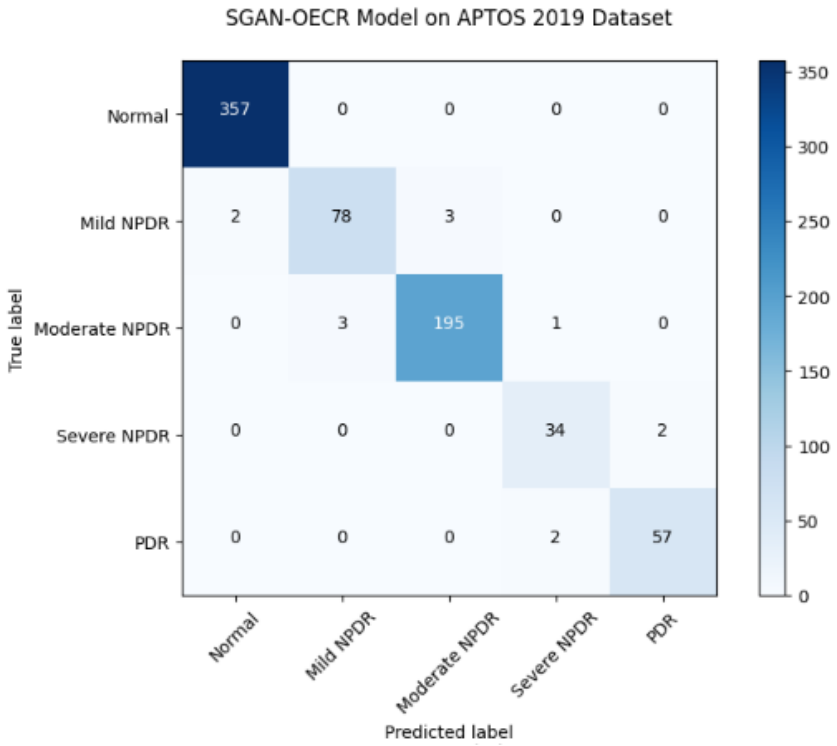

Figure 7.4: Confusion matrix for SGAN-OECR model on the APTOS 2019 dataset

Figure 7.5 illustrates the comparison of performance metrics versus population size for the SGAN-OECR model on the APTOS dataset. The results are analyzed by varying the population size. The plot shows that when the population size increases, there is an improvement in the performance metrics such as accuracy, precision, recall and F1-score. For the population size of 20, the performance metrics are efficient compared to the other population sizes.

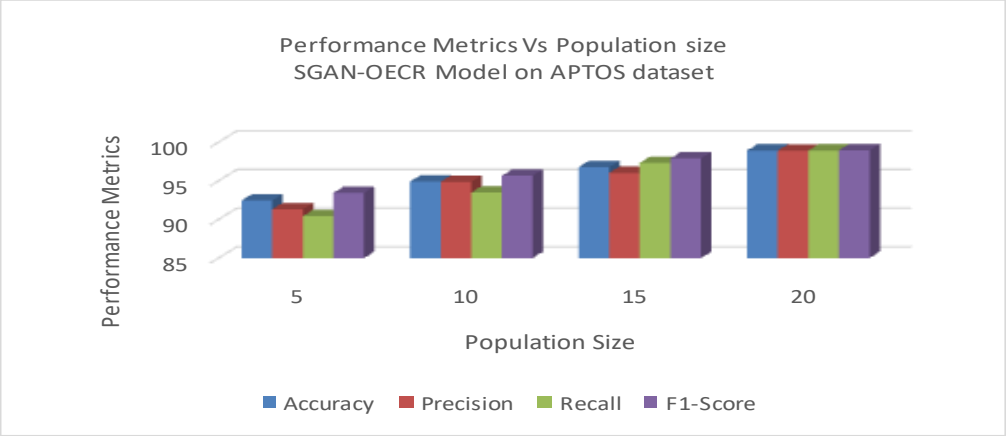

Figure 7.5: Performance Metrics Vs. Population size for SGAN-OECR model on APTOS 2019 dataset

7.3.2 Result Analysis of SGAN-OECR model on the IDRiD dataset

Multi-class classification is performed on the IDRiD dataset, and it is classified into five classes starting from 0 to 4. In the IDRiD dataset, out of 516 training samples, 20% of the samples are considered for test data.

Table 7.5 illustrates the existing models for DR Stage classification on the IDRiD dataset. Table 7.6 shows the comparison of the proposed models for DR Stage classification on the IDRiD dataset. Accuracy metric is one of the frequently used metrics, and the other metrics are presented. The accuracy percentage obtained by the MSA-ResNetGB is 94.18 and SGAN-ECR is 96.12. The accuracy percentage obtained by the SGAN-OECR model is 97.09, which is superior to that of the existing models.

Figure 7.6 shows the SGAN-OECR model's confusion matrix on the IDRiD dataset. The matrix illustrates the distribution of samples by classes and the ratio of accurate classification and misclassified samples. For example, the precisely identified sample count is 34 for class 0 (no DR). For class 1(mild DR), the precisely identified sample count is 3. For

class 2 (moderate DR), the precisely identified sample count is 31. For class 3(Severe DR), the precisely identified sample count is 13 and finally, for class 4 (PDR), the precisely identified sample count is 19.

Table 7.5: Existing models for DR Stage Classification on the IDRiD dataset

Reference	Classification Technique	Accuracy (%)	Precision (%)	Recall (%)	F1-Score (%)
Hemanth D *et al.* (2020)	CNN Model	86.02	89.67	90.24	91.93
Bilal A *et al.* (2021)	Mixed Model	87.50	91.76	93.38	92.86
Saeed F *et al.* (2021)	ResNetGB	88.89	93.51	93.51	93.51
Tariq H *et al.* (2022)	DTL Model	89.01	93.83	93.83	93.83
Alimanov A *et al.* (2022)	CBAM-UNet	89.47	94.94	92.59	93.75
Butt M *et al.* (2022)	HDL Model	90.11	93.83	95.00	94.41

Table 7.6: Comparison of the Proposed Models for DR Stage Classification on the IDRiD dataset

Reference	Classification Technique	Accuracy (%)	Precision (%)	Recall (%)	F1-Score (%)
SrinivasanV & Rajagopal V (2022)	MSA-ResNetGB Model	94.18	91.48	91.57	91.45
Valarmathi S and Vijayabhanu R (2022)	SGAN-ECR model	96.12	96.31	93.73	94.77
Valarmathi Srinivasan & Vijayabhanu Rajagopal (Proposed - 2023)	**SGAN-OECR Model**	**97.09**	**97.37**	**96.42**	**96.86**

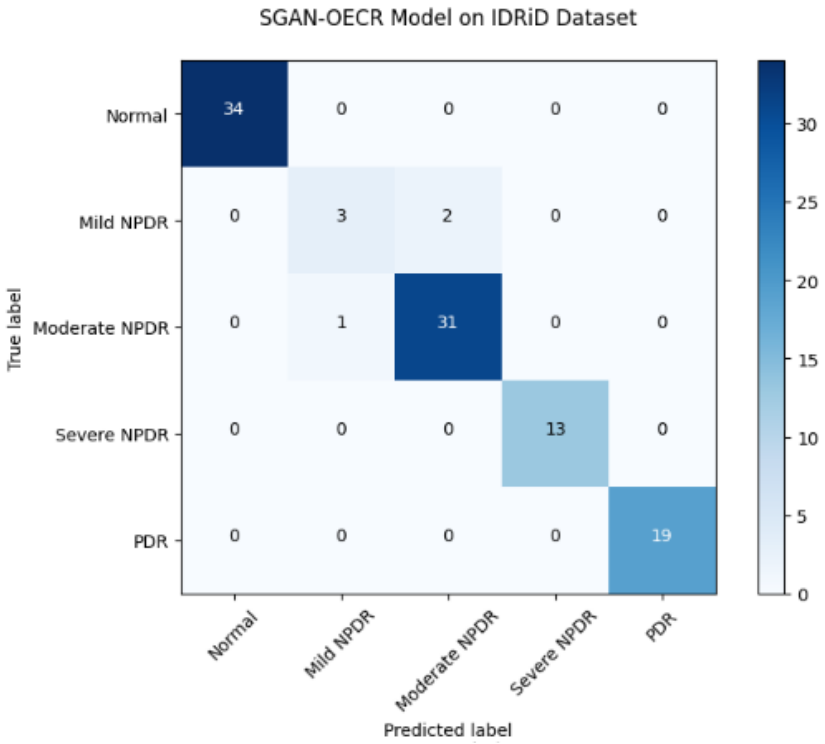

Figure 7.6: Confusion matrix for SGAN-OECR model on the IDRiD dataset

The error rate can be minimized when there is an optimized parameter selection for the classifiers in the architecture model. The average error rate between the restored and the original image is depicted in Figure 7.7. If the MSE values are low, more optimal solutions will be obtained. This process eliminated overfitting and training effectiveness is maximized by decreasing the parameter count. An optimal variable choice aids in efficiency of the training model and its convergence.

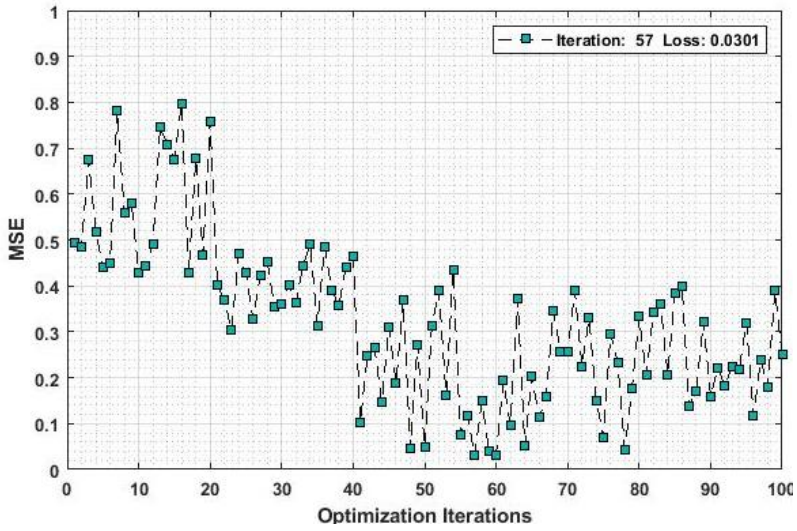

Figure 7.7: MSE vs. Optimization Iterations

Figure 7.8 illustrates the comparison of performance metrics versus population size for the SGAN-OECR model on the IDRiD dataset. The results are analyzed by varying the population size. The plot shows that when the population size increases, there is an improvement in the performance metrics such as accuracy, precision, recall and F1-score. For the population size of 20, the performance metrics are efficient compared to the other population sizes.

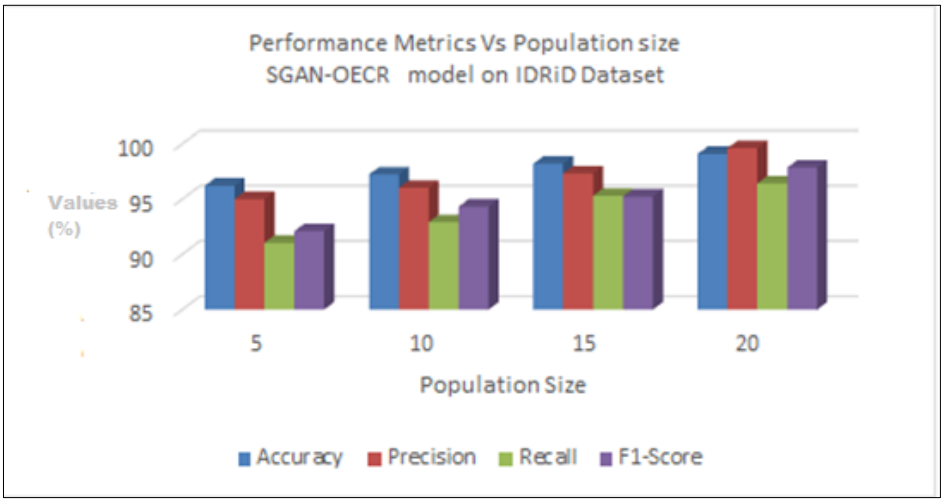

Figure 7.8: Performance Metrics Vs. Population size for SGAN-OECR model on the IDRiD dataset

Table 7.7 illustrates the tuned hyper-parameter values of the MSA-ResNet structure on the APTOS and IDRiD datasets. The proposed model aids in predicting optimized hyper-parameter values based on the selection of the training model. The amount of training data is increased gradually in each iteration while the accuracy of the model is enhanced rapidly. Finally, an optimized set of hyper-parameters is obtained.

Table 7.7: Tuned Hyper-parameter values of MSA-ResNet structure on the APTOS and IDRiD Dataset

S.No.	Hyper-parameters	APTOS Tuned value	IDRiD Tuned value
1	Learning Rate	0.077	0.005
2	Momentum	0.96	0.95
3	Batch size	64	64
4	Convolutional Layer	256	128
5	Kernel size	(3,3)	(3,3)
6	Activation function	ReLU	ReLU
7	Filter size	128	64
8	No. of epochs	80	100

7.3.3 Results obtained from the SGAN-OECR model

This section analyses the results obtained by the SGAN-OECR model. The results obtained by the proposed SGAN-OECR model were applied to the APTOS and IDRiD datasets, and it outperforms the literature models. Table 7.8 compares the performance of the SGAN-OECR model on the APTOS and IDRiD datasets. The SGAN-OECR model on the APTOS dataset achieved 98.21% accuracy, 98.12% precision, 96.42% recall, and 97.86% F1-Score. The SGAN-OECR model on the IDRiD dataset has obtained 97.09% accuracy, 97.37% precision, 96.42% recall, and 96.86% F1-Score. The performance of the APTOS dataset exceeds the performance of the IDRiD dataset. When both the datasets are compared, the occurrence of performance loss in IDRiD dataset is due to shortage of samples.

Table 7.8: Performance Comparison of SGAN-OECR model on APTOS and IDRiD dataset

Dataset	Accuracy (%)	Precision (%)	Recall (%)	F1-Score (%)
APTOS	98.21	98.12	96.42	97.86
IDRiD	97.09	97.37	96.42	96.86

The proposed SGAN-OECR model's training ability is represented in Figure 7.9, which shows the accuracy plot for the SGAN-OECR model on both APTOS and IDRiD datasets. The model accuracy increases when the number of iterations increases. Figure 7.10 shows the loss plot for the proposed model that is a good fit for both APTOS and IDRiD datasets. The training loss drops at a point of constancy that is optimal for the model. The average execution time (in seconds) of the proposed SGAN-OECR model model is 1.69 for APTOS dataset and 1.72 for IDRiD dataset.

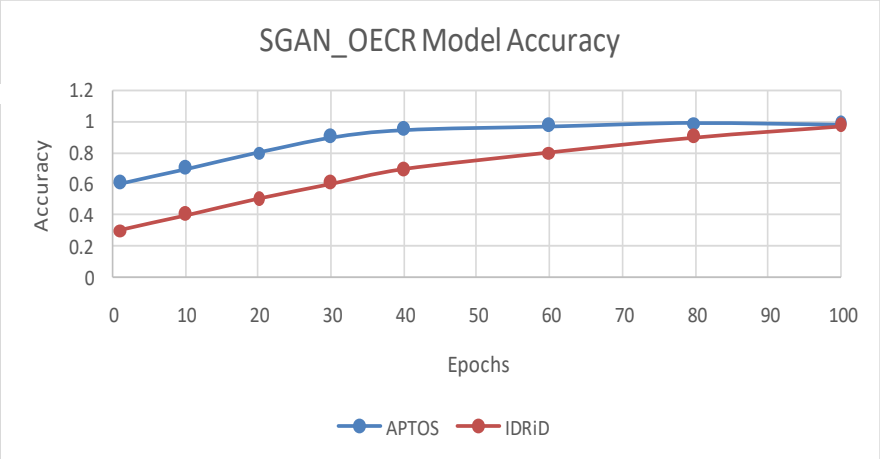

Figure 7.9: SGAN-OECR model Accuracy Plot

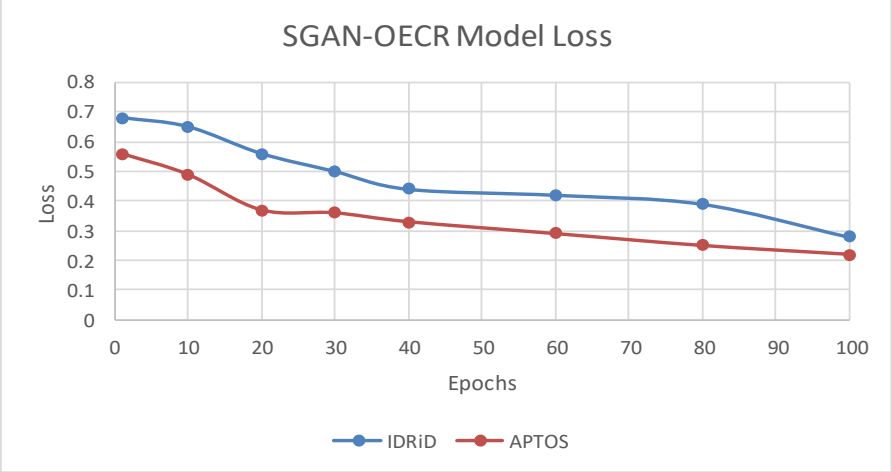

Figure 7.10: SGAN-OECR model Loss Plot

Table 7.9 represents the performance metrics of the SGAN-OECR model with and without preprocessing on the APTOS datasets. The performance metrics of the SGAN-OECR model without preprocessing produce better results compared to the results produced with preprocessing.

Table 7.9: Performance of SGAN-OECR model with and without preprocessing on the APTOS dataset

Metric	SGAN-OECR Model with Preprocessing	SGAN-OECR Model without Preprocessing
Accuracy (%)	90.09	**98.21**
Precision (%)	89.69	**98.12**
Recall (%)	89.36	**96.42**
F1-Score (%)	89.01	**97.86**

Table 7.10 represents the performance metrics of the SGAN-OECR model with and without preprocessing on the IDRiD datasets. The performance metrics of the SGAN-OECR model without preprocessing produce better results compared to the results produced with preprocessing. The SGAN-ECR and SGAN-OECR models perform well when SGAN-augmented images are used for training. On the other hand, when pre-processed images, i.e., greyscale images, are used, the models start to underperform. This is because SGAN generates high-contrast RGB images, which in turn produce better performance when it is

used for training the model. The performance metrics of the SGAN-OECR model without preprocessing produce better results for the APTOS and IDRiD datasets.

Table 7.10: Performance of SGAN-OECR model with and without preprocessing on IDRiD dataset

Metric	SGAN-OECR Model with preprocessing	SGAN-OECR Model without preprocessing
Accuracy (%)	84.36	**97.09**
Precision (%)	83.94	**97.37**
Recall (%)	84.19	**96.42**
F1-Score (%)	83.67	**96.86**

Figure 7.11 shows the ROC curve plot for the proposed SGAN-OECR model as an evaluation metrics for the APTOS datasets. The ROC curve for all the classes 0-4 lies closer to 1, indicating that the SGAN-OECR model performs well on the APTOS dataset.

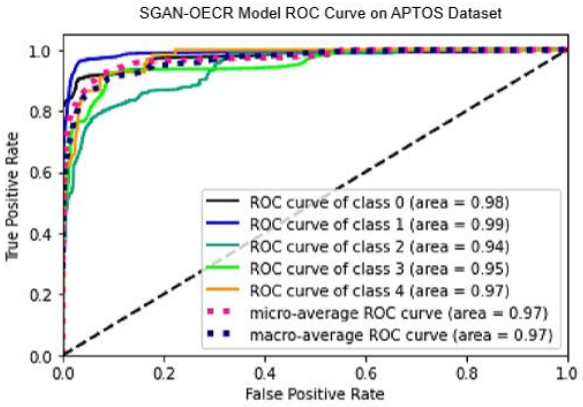

Figure 7.11: ROC Curve Plot for APTOS dataset

Figure 7.12 shows the ROC curve plot for the proposed SGAN-OECR model as evaluation metrics for the IDRiD datasets. The ROC curve for all classes (0-4) lies closer to 1, indicating that the SGAN-OECR model performs well on the IDRiD dataset, but its performance is not as high when compared to the results on the APTOS dataset.

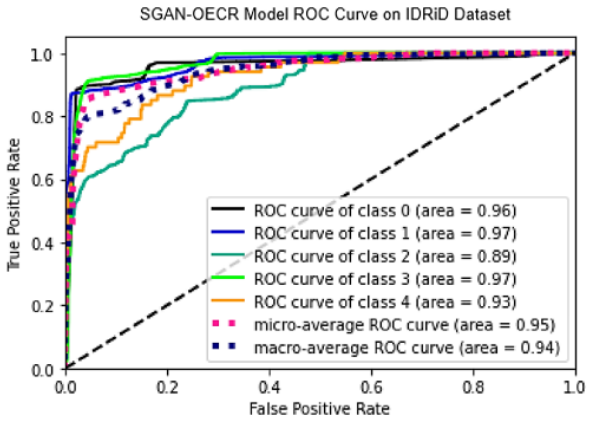

Figure 7.12: ROC Curve Plot for IDRiD dataset

7.4 Summary

In this chapter, SGAN-OECR model was proposed to improve the performance of DR stage classification. Initially, the MSA-ResNet architecture is computed using a binary encoding process. Every layer in the CNN model consists of a hyper-parameter set which are encoded in other layers. Later, the hyper-parameters are optimized using the EMBOA to enhance MSA-ResNet. Fitness function estimates the classification enhancement of DR lesions with deformities. The proposed model automatically assigns the values of the hyper-parameters in the MSA-ResNet architecture for classifying the DR stages. Experimental results are validated and analyzed based on the performance metrics, the outcome analysis and assessment of the proposed technique are compared with the literature work. Thus, the accuracy of 98.21% and 97.09% is achieved in the SGAN-OECR model on APTOS and IDRiD datasets compared to the existing classification models for DR stage classification.